Video Article

Synthesis and Functionalization of 3D Nano-graphene Materials: Graphene Aerogels and Graphene Macro Assemblies

Patrick G. Campbell[1], Marcus A. Worsley[1], Anna M. Hiszpanski[1], Theodore F. Baumann[1], Juergen Biener[1]

[1]Materials Science Division, Lawrence Livermore National Laboratory

Correspondence to: Patrick G. Campbell at campbell82@llnl.gov

URL: https://www.jove.com/video/53235
DOI: doi:10.3791/53235

Keywords: Engineering, Issue 105, Graphene, sol-gel, aerogel, carbon nanotube, supercapacitor, battery, electrode, low density, high surface area

Date Published: 11/5/2015

Citation: Campbell, P.G., Worsley, M.A., Hiszpanski, A.M., Baumann, T.F., Biener, J. Synthesis and Functionalization of 3D Nano-graphene Materials: Graphene Aerogels and Graphene Macro Assemblies. *J. Vis. Exp.* (105), e53235, doi:10.3791/53235 (2015).

Abstract

Efforts to assemble graphene into three-dimensional monolithic structures have been hampered by the high cost and poor processability of graphene. Additionally, most reported graphene assemblies are held together through physical interactions (*e.g.*, van der Waals forces) rather than chemical bonds, which limit their mechanical strength and conductivity. This video method details recently developed strategies to fabricate mass-producible, graphene-based bulk materials derived from either polymer foams or single layer graphene oxide. These materials consist primarily of individual graphene sheets connected through covalently bound carbon linkers. They maintain the favorable properties of graphene such as high surface area and high electrical and thermal conductivity, combined with tunable pore morphology and exceptional mechanical strength and elasticity. This flexible synthetic method can be extended to the fabrication of polymer/carbon nanotube (CNT) and polymer/graphene oxide (GO) composite materials. Furthermore, additional post-synthetic functionalization with anthraquinone is described, which enables a dramatic increase in charge storage performance in supercapacitor applications.

Video Link

The video component of this article can be found at https://www.jove.com/video/53235/

Introduction

Since the isolation of graphene in 2004,[1] interest in harnessing its unique properties has led to intense effort directed toward assembling graphene into three-dimensional, monolithic structures that retain the properties of individual graphene sheets.[2-5] These efforts have been hampered by the fact that graphene itself is expensive and time consuming to produce and tends to aggregate in solution, which limits the scalability of materials based on graphene building blocks. Additionally, graphene assemblies are typically comprised of physical cross-linking interactions (*e.g.*, van der Walls forces) between the individual graphene sheets, which are much less conductive and mechanically robust than chemical bond cross-links. Lawrence Livermore National Laboratory has been involved in the development of novel porous, low-density carbon materials since the 1980s.[6] Several strategies have been identified to fabricate mass-producible graphene-based monolithic bulk materials from both low-cost polymer-derived carbon foams, which are called graphene aerogels (GAs),[7] as well as by direct cross-linking of graphene oxide (GO) sheets, which are called graphene macro-assemblies (GMAs).[8,9] These ultrahigh surface area bulk materials have high electrical and thermal conductivities, exceptional mechanical strength and elasticity, and tunable pore morphologies. GAs and GMAs have found utility in numerous applications including electrode materials in supercapacitors and rechargeable batteries, advanced catalyst supports, adsorbents, thermal insulation, sensors, and desalinization.[10]

The synthesis of graphene aerogels begins with sol-gel polymerization of an aqueous solution of resorcinol and formaldehyde to generate highly cross-linked organic gels. These gels are washed with water and acetone, then dried using supercritical CO_2 and pyrolyzed in an inert atmosphere to give carbon aerogels with relatively low surface area and pore volume. Carbon aerogels are activated by controlled removal of carbon atoms under mild oxidizing condition (*e.g.*, CO_2) to form a cross-linked material composed of both amorphous carbon and graphite nanoplatelets, with higher surface area and open pore morphology.[7] A unique advantage of the sol-gel synthesis is that GAs can be fabricated in a variety of forms, including monoliths and thin films, depending on the needs of the application. Carbon nanotubes[11] and/or graphene sheets[12] can be integrated into GAs by including these additives in the sol-gel precursor solution. This generates composite structures in which the additive becomes a part of the primary carbon network structure. Additionally, the GA framework can be functionalized after carbonization/activation either through modification of the aerogel surface or through the deposition of materials, for example catalyst nanoparticles, onto the framework structure.[13]

Graphene macro-assemblies (GMAs) are prepared by directly cross-linking suspended graphene oxide (GO) sheets, taking advantage of their inherent chemical functionality.[9] GO sheets contain a variety of functional groups, including epoxide and hydroxide moieties, that can serve as chemical cross-linking sites. As in the GA preparation, assembled GMAs are supercritically dried to preserve the porous network, then pyrolized to reduce the chemical cross-links into conductive carbon bridges that provide structural support for the assembly. Due to the covalent carbon bridges between graphene sheets, GMAs have electrical conductivities and mechanical stiffness that are orders of magnitude higher than graphene assemblies formed with physical cross-linking. Additionally, GMAs have surface areas approaching the theoretical value of a single

graphene sheet. Post-synthetic thermal treatment at elevated temperatures (>1,050 °C) can significantly improve the crystallinity of GMAs, leading to even higher conductivities and Young's moduli as well as better thermal oxidation resistance.[14] Post-synthetic chemical treatment of GMAs with redox-active organic molecules such as anthraquinone can enhance charge storage capacity in supercapacitor applications.[15]

The tunable material properties of GAs and GMAs are, in part, a result of carefully varying synthetic conditions such as reagent and catalyst concentrations, cure time and temperature, drying conditions, and carbonization/activation processes.[16] This detailed video protocol aims to resolve ambiguities in the published methods, and to guide researchers attempting to reproduce the materials and conditions.

Protocol

1. Resorcinol-formaldehyde (RF) Derived Graphene Aerogels

1. Na_2CO_3 catalyzed carbon aerogel (11% solids, cRF)
    1. In a 40 ml scintillation vial, add deionized water (7.1 ml) to resorcinol (0.625 g, 5.68 mmol) and mix on a vortex for 1 min. Crush large resorcinol pieces to powder using a mortar and pestle prior to water addition. Note that they may not completely dissolve until the next step.
    2. Add 37% formaldehyde solution (0.900 g, 11.4 mmol) to the resorcinol slurry and vortex for 1 min.
    3. Add sodium carbonate (0.003 g, 0.028 mmol) to the reaction mixture and vortex for 1 min.
    4. Transfer the reaction mixture to glass molds that can be sealed air tight (*e.g.*, vial or glass slides that are separated by a silicone gasket) which define the shape of the resulting solid part.
    5. Place the sealed molds into an 80 °C oven and cure for 72 hr.
    6. After curing, remove the solid monoliths from the glass mold and wash with water to remove residual unreacted starting materials and catalyst. Typically we perform 3 x 12 hr washes with fresh DI H_2O. The material is now ready for drying.

2. Acetic acid catalyzed carbon aerogel (AARF)[17]
    1. In a 40 ml scintillation vial, add deionized water (15 ml) to resorcinol (12.3 g, 0.112 mol) and mix on a vortex for 1 min. Crush large resorcinol pieces to powder using a mortar and pestle prior to water addition. Note that they may not completely dissolve until the next step.
    2. Add 37% formaldehyde solution (17.9 g, 0.224 mol) to the resorcinol slurry and vortex for 1 min.
    3. Add glacial acetic acid (0.44 g, 0.007 mol) to the reaction mixture and vortex for 1 min.
    4. Transfer the reaction mixture to glass molds that can be sealed air tight (*e.g.*, vial or glass slides that are separated by a silicone gasket), which define the shape of the resulting solid part.
    5. Place the sealed molds into an 80 °C oven and cure for 72 hr.
    6. After curing, remove the solid monoliths from the glass mold and wash with water to remove residual unreacted starting materials and catalyst. Typically we perform 3 x 12 hr washes with fresh DI H_2O. The material is now ready for drying.

3. Carbon Additives to the RF precursor solution (CNT, GO)
    1. Carbon nanotube/RF composite[11]
        1. Suspend 1 wt% single-walled carbon nano-tubes in deionized water and thoroughly disperse using an ultrasonic bath (sonic power 90 W, frequency 40 kHz).
        2. Add resorcinol (1.235 g, 11.2 mmol), formaldehyde (1.791 g, 22.1 mmol), and sodium carbonate catalyst (5.95 mg, 0.056 mmol) to 1.5 g of the CNT dispersion.
        3. Transfer the reaction mixture to glass molds that can be sealed air tight (*e.g.*, vial or glass slides that are separated by a silicone gasket), which define the shape of the resulting solid part.
        4. Place the sealed molds into an 80 °C oven and cure for 72 hr.
        5. After curing, remove the solid monoliths from the glass mold and wash with water to remove residual unreacted starting materials and catalyst. Typically perform 3 x 12 hr washes with fresh DI H_2O. The material is now ready for drying.
    2. Graphene oxide/RF composite[12]
        1. Suspend 1 wt% graphene oxide (GO, 300-800 nm diameter) in deionized water and thoroughly disperse using an ultrasonic bath (sonic power 90 W, frequency 40 kHz).
        2. Add resorcinol (1.235 g, 11.2 mmol), formaldehyde (1.791 g, 22.1 mmol, 37% solution) and sodium carbonate catalyst (5.95 mg, 0.056 mmol) to 1.5 g of the GO dispersion.
        3. Transfer the reaction mixture to glass molds that can be sealed air tight (*e.g.*, vial or glass slides that are separated by a silicone gasket) which define the shape of the resulting solid part.
        4. Place the sealed molds into an 80 °C oven and cure for 72 hr.
        5. After curing, remove the solid monoliths from the glass mold and wash with water to remove residual unreacted starting materials and catalyst. Typically perform 3 x 12 hr washes with fresh DI H_2O. The material is now ready for drying.

4. Drying
    1. Supercritical CO_2
        1. Prepare washed samples for drying with supercritical CO_2 by exchanging the H_2O solvent with acetone. Remove sample from water bath and place into bath containing clean acetone. Replace with fresh acetone two more times at 12 hr intervals.
        2. Load acetone-exchanged samples into a supercritical drying apparatus, filled with acetone and with circulating coolant at 12-15 °C.
        3. Seal supercritical dryer and exchange with liquid CO_2 until no acetone remains (4-24 hr depending on sample size, density, pore morphology, *etc.*).

4. Shut off CO_2 supply and raise temperature of circulating coolant to 55 °C, while maintaining pressure in the supercritical dryer between 1,200-1,600 psi (80-110 bar). Hold at 55 °C for 1 hr.
5. Slowly vent CO_2 (2-12 hr) while maintaining temperature of circulating coolant at 55 °C. Remove samples.

2. Ambient drying (Xerogel)
    1. Prepare washed samples for drying under ambient conditions by exchanging the H_2O solvent with acetone. Remove sample from water bath and place into bath containing clean acetone. Replace with fresh acetone two more times at 12 hr intervals.
    2. Place acetone-exchanged samples on a clean surface (*e.g.*, Teflon block). To slow the rate of solvent evaporation to prevent cracking and uneven shrinking, cover the sample with an inverted beaker of sufficient volume to provide plenty of headspace.
    3. Allow solvent to evaporate for (24-72 hr).

5. Carbonization
    1. Perform carbonization of the dried foams at 1,050 °C under N_2 atmosphere. Ramp from RT at a rate of 5 °C/min, and hold at 1,050 °C for 3 hr. Note that thin samples may need to be placed between two sheets of graphite paper (or other temperature stable, non-reactive material) with weight on top to prevent curling and "potato chipping."

6. Activation
    1. Activate an AARF carbon foam part (2 cm × 3 cm × 4 mm, 1.2 g) to generate 3D nanographene (3D-NG) under flowing CO_2 (10 sccm) at 950 °C for 5 hr.[7]

2. Graphene Oxide Derived Graphene Macro Assemblies

1. NH_4OH catalyzed GO assembly
    1. In a 40 ml scintillation vial, add deionized water (20 ml) to 400 mg single layer graphene oxide (GO, 300-800 nm diameter). Thoroughly disperse using an ultrasonic bath (sonic power 90 W, frequency 40 kHz) O/N.
    2. Add concentrated NH_4OH solution (0.211 ml per g GO suspension).
    3. Transfer into glass molds that can be sealed airtight (*e.g.*, vial or glass slides that are separated by a silicone gasket which defines the shape of the resulting solid part).
    4. Place the sealed molds into an 80 °C oven and cure for 72 hr.
    5. After curing, remove the solid monoliths from the glass mold and wash with water to remove residual unreacted starting materials and catalyst. Typically perform 3 x 12 hr washes with fresh DI H_2O. The material is now ready for drying.

2. Drying
    1. Supercritical CO_2
        1. Prepare washed samples for drying with supercritical CO_2 by exchanging the H_2O solvent with acetone. Remove sample from water bath and place into bath containing clean acetone. Replace with fresh acetone two more times at 12 hr intervals.
        2. Load acetone-exchanged samples into a supercritical drying apparatus, filled with acetone and with circulating coolant at 12-15 °C.
        3. Seal supercritical dryer and exchange with liquid CO_2 until no acetone remains (4-24 hr depending on sample size, density, pore morphology, *etc.*). Complete exchange is indicated by cessation of acetone drips at the exhaust valve of the supercritical dryer.
        4. Shut off CO_2 supply and raise temperature of circulating coolant to 55 °C, while maintaining pressure in the supercritical dryer between 1,200-1,600 psi (80-110 bar). Hold at 55 °C for 1 hr.
        5. Slowly vent CO_2 (2-12 hr) while maintaining temperature of circulating coolant at 55 °C. Remove samples.

    2. Ambient drying (xerogel)
    Note that thin samples may need to be placed between two sheets of Teflon (or other non-stick material) with weight on top to prevent curling and "potato chipping."
        1. Prepare washed samples for drying under ambient conditions by exchanging the H_2O solvent with acetone. Remove sample from water bath and place into bath containing clean acetone. Replace with fresh acetone two more times at 12 hr intervals.
        2. Place acetone-exchanged samples on a clean surface (*e.g.*, Teflon block). To slow the rate of solvent evaporation to prevent cracking and uneven shrinking, cover the sample with an inverted beaker of sufficient volume to provide plenty of headspace.
        3. Allow solvent to evaporate for (24-72 hr).

3. Carbonization
    1. Perform carbonization of the dried foams at 1,050 °C under N_2 atmosphere. Ramp from RT at a rate of 5 °C/min, and hold at 1,050 °C for 3 hr. Note that thin samples may need to be placed between two sheets of graphite paper (or other temperature stable, non-reactive material) with weight on top to prevent curling and "potato chipping."
    2. Thermal anneal for highly crystalline GMA. Perform additional thermal annealing of carbonized foams at temperatures up to 2,500 °C under He atmosphere. Ramp from RT at a rate of 100 °C/min, and hold at elevated temperature for 1 hr.

4. Post-carbonization functionalization
    1. Non-covalent anthraquinone functionalization (AQ-GMA)
        1. Prepare a 3 mM solution of anthraquinone (AQ) in dry EtOH. Heat in a sealed vial at 75 °C to ensure complete dissolution.
        2. Add hot AQ solution to GMA sample (~2 ml/mg of sample). Soak in a sealed vial for 2 hr at 75 °C.
        3. Remove excess AQ solution from vial and allow sample to dry at 75 °C O/N (vial cap off).

Representative Results

The evolution of material composition and morphology during fabrication can be tracked in various ways including X-ray diffraction, Raman and NMR spectroscopy, electron microscopy, and porosimetry. For example, in the synthesis, pyrolysis, and CO_2 activation of GAs, the conversion was followed by X-ray diffraction (XRD) (**Figure 1E**). The absence of the stacking-related (002) diffraction peak in the XRD pattern after activation (blue trace) indicates the transition from a structure containing graphite nanoplatelets to one consisting of single-layer graphene. Scanning electron microscopy (SEM) and high-resolution transmission electron microscopy (HRTEM) revealed short, linear features, which could be identified as individual graphene sheets viewed edge-on (**Figure 1C** and **D**). The Raman features for GA are similar to those observed for commercial graphene samples grown by chemical vapor deposition (**Figure 1F**). Solid state nuclear magnetic resonance (NMR) was used to follow the transformation of GO into GMA (**Figure 2**),[9] which reveals that the significant epoxide and hydroxyl functionality (peaks between 50 and 75 ppm), as well as carbonyl groups (168 ppm) in its ^{13}C NMR spectrum are virtually eliminated after curing, and an aliphatic carbon peak (26 ppm) appears, which suggests that epoxide and hydroxyl groups are involved in the cross-linking mechanism. After pyrolysis/carbonization, only the sp^2 carbon peak remains and the ^1H NMR spectrum (**Figure 2B**) also shows the elimination of–CH_2– and –CH_2O– moieties suggesting that the sp3 carbon cross-links were thermally converted to conductive sp^2 carbon junctions. The GMA microstructure was analyzed by SEM and appears similar to that reported in other graphene assemblies (**Figure 3**). The nitrogen porosimetry adsorption/desorption isotherm shown in **Figure 4A** is Type IV, indicative of a mesoporous material. Post synthetic modification of GMA with anthraquinone was characterized by thermogravimetric analysis (TGA), with representative isotherms presented in **Figures 5B** and **C**. The derivatives of the mass loss curves show peaks at different temperatures for AQ-GMA and bulk AQ due to the adsorption of the AQ molecule on the carbon substrate. Electrochemical characterization included cyclic voltammetry (CV), which shows that AQ adsorption onto the GMA electrode produced reversible and stable faradaic charge storage (**Figure 6A**).

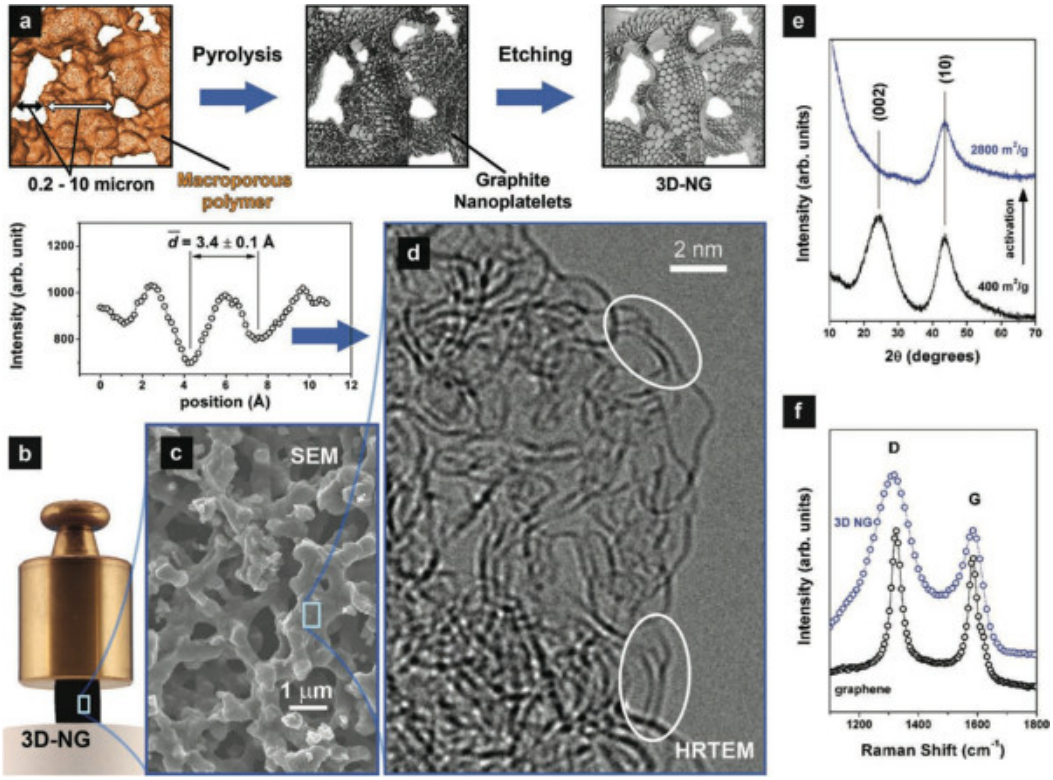

Figure 1. Processing and architecture of 3D-NG (GA). (**A**) Schematic of the polymer-based top-down approach. (**B**) Illustration of the mechanical robustness of a centimeter-sized 3D-NG sample. (**C**) Open macroporous network architecture composed of micrometer-sized pores and ligaments. (**D**) Internal structure of ligaments composed of curved and intertwined graphene sheets. Selected double-layer regions are marked by ovals, and a typical intensity profile across such a double-layer region is shown on the left. (**E**) X-ray diffraction data confirming the transformation of the initial multilayer graphene component to one that is dominated by single-layer graphene. (**F**) Comparison of the Raman spectra in the D/G band region from 3D-NG and multiple- layer graphene. This figure has been modified from Ref. 7. Please click here to view a larger version of this figure.

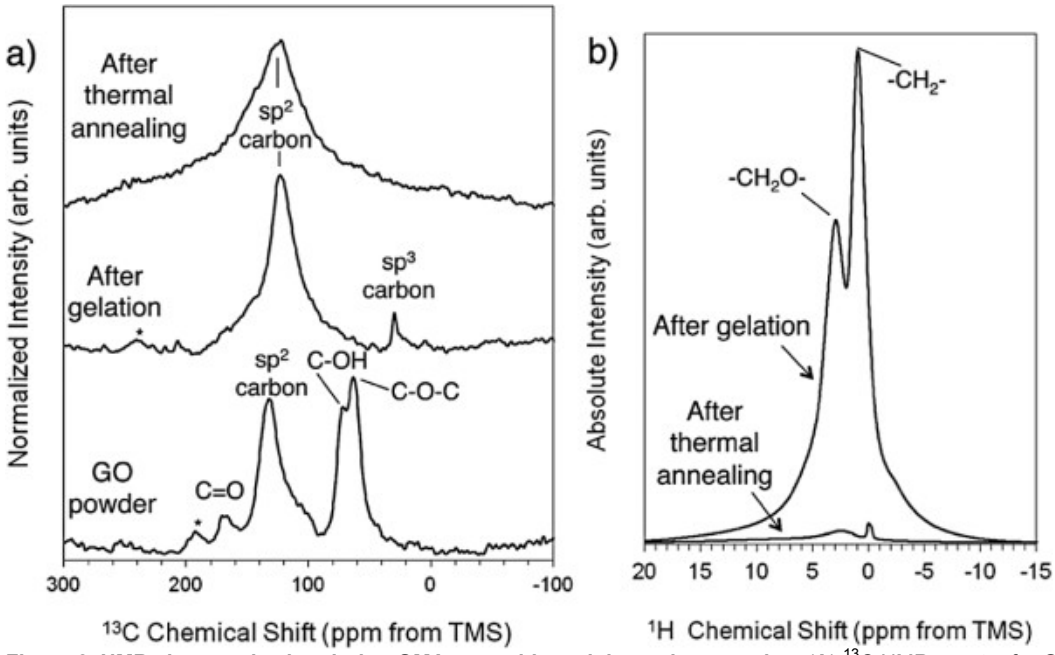

Figure 2. NMR characterization during GMA assembly and thermal processing. (**A**) ^{13}C NMR spectra for GO powder, GO after initial gelation, and 3D graphene macroassembly. (**B**) ^{1}H NMR spectra for GMA before and after thermal annealing. This figure has been modified from Ref. 9. Please click here to view a larger version of this figure.

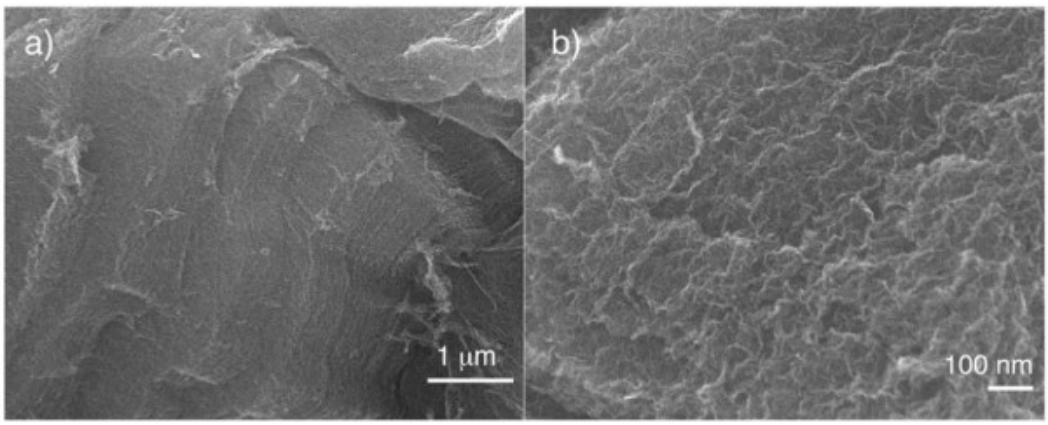

Figure 3. FE-SEM images of the fracture surface of the 3D graphene macroassembly. (**A**) Low magnification. (**B**) High magnification. This figure has been modified from Ref. 9. Please click here to view a larger version of this figure.

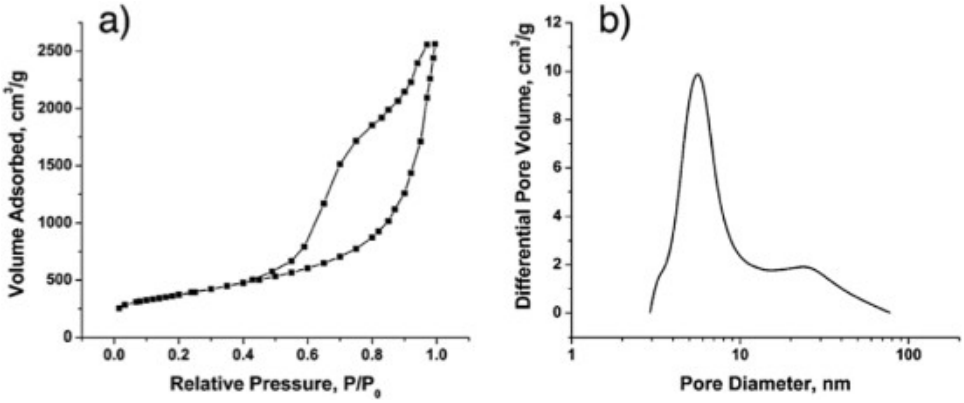

Figure 4. Pore morphology of GMAs. (**A**) Nitrogen adsorption/desorption isotherm. (**B**) Pore size distribution. This figure has been modified from Ref. 9. Please click here to view a larger version of this figure.

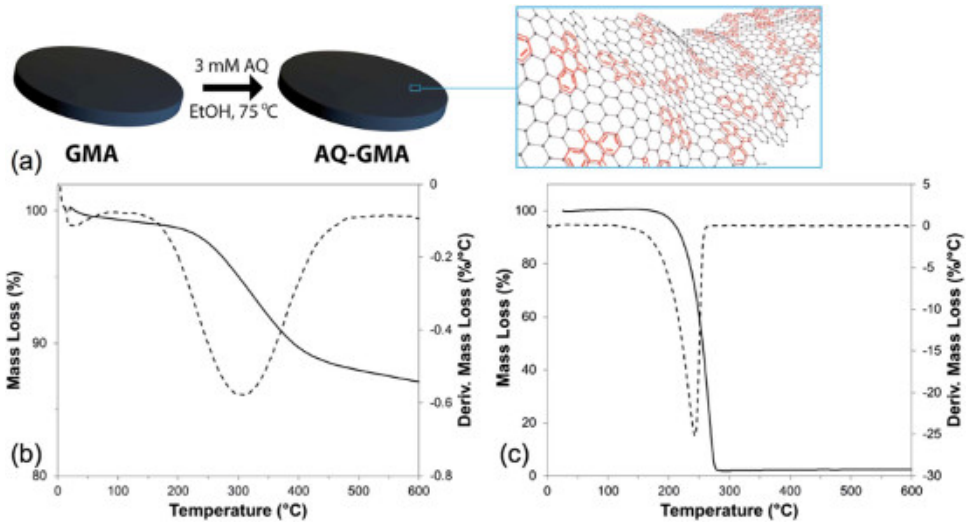

Figure 5. Synthesis and characterization of AQ-GMAs. (**A**) Synthetic procedure and schematic illustration of non-covalent AQ functionalization of GMA electrodes. (**B**) TGA curve for 250 mm thick AQ-GMA disk with 11.2 wt% AQ loading (10.1% of total mass) and (**C**) TGA curve for bulk AQ (Ar flow 10 ml min^{-1}, 10 °C min^{-1} temperature ramp). Derivative mass loss curves (dashed lines) show peaks at different temperatures for the AQ-GMA vs. bulk AQ. A higher temperature of more than 60 °C indicates adsorption of the AQ molecules on the carbon substrate. This figure has been modified from Ref. 15. Please click here to view a larger version of this figure.

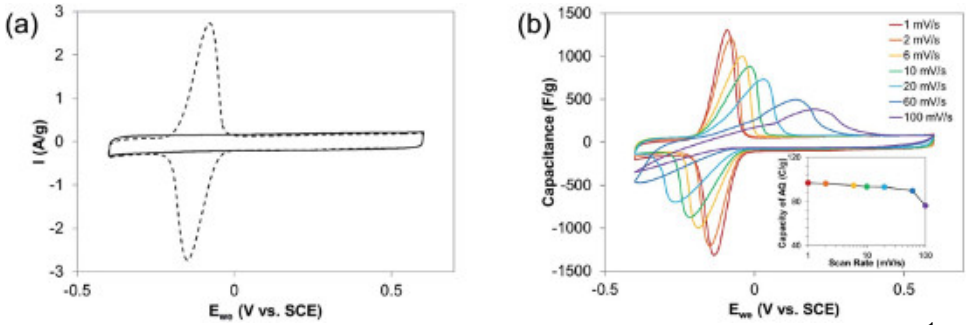

Figure 6. Electrochemical characterization of AQ-GMAs. (**A**) Cyclic voltammogram (2 mV sec^{-1}, 1 M HCl) for 250 mm thick GMA disks, as prepared (solid line), and with 12.4 wt% AQ loading (dashed line). (**B**) CVs of the same 12.4 wt% AQ-GMA sample at different potential sweep rates. The inset plot illustrates that AQ contribution to charge storage capacity remains constant until >60 mV sec^{-1}, where solution resistance causes such large overpotentials that AQ cannot fully charge within the applied voltage window. (Capacity values were derived by integrating the discharge peak associated with AQ and subtracting underlying capacity of GMA.) This figure has been modified from Ref. 15. Please click here to view a larger version of this figure.

Discussion

It is important to note that the procedures outlined here are only representative. Many adjustments are possible to tune materials for a specific application. For example, varying the starting material concentrations, while keeping resorcinol/formaldehyde (RF) ratio constant, can have an impact on the final material density. Catalyst loading can alter pore morphology, as a higher loading in the RF procedure leads to smaller primary particles and vice-versa. Activation time can play a role as well; at shorter activation times, new porosity is generated in the form of micropores while at longer activation times micropores are widened to sizes that cross the micropore–mesopore boundary.[15] Additionally, the activation time must take into consideration the weight of the starting carbon foam; typical yields from the activation process described above were *ca.* 25%–30%, based on the weight of the starting carbon foam.

The same types of adjustments can be made with regard to additives such as CNTs and GO to the RF starting solution. Using the general techniques described above, foams with CNT loadings ranging from 0 to 60 wt% (with respect to RF solids) were prepared. The highest conductivity graphene aerogel achieved with this method used 1 wt% GO and 4 wt% RF in the initial reaction mixture; use of higher RF:GO ratios resulted in lower conductivity values. Graphene macroassemblies are generally limited to initial concentrations of ≤20 mg/ml because it is difficult to achieve stable suspensions at higher concentrations; suspensions of less than 10 mg/ml will still form monolithic structures, however they shrink considerably upon curing and carbonization making very low density materials difficult to achieve through initial concentration alone.

Carbonization temperature also provides opportunities for material tuning. Electrical conductivity increases dramatically above 800 °C for RF based materials. At carbonization temperatures above 1,500 °C, GMAs lose surface area and become more graphitic, with fewer defects in the graphene sheets.

In contrast to the flexibility in the material synthesis described above, we found that when functionalizing the GMA materials with anthraquinone, increased concentration and longer soak times did not result in higher AQ loading. This can be attributed to roughly monolayer AQ coverage, with layers beyond the first lacking stabilizing van der Waals interactions with the GMA substrate.

Future applications of the synthetic protocol described here include incorporating sacrificial templates into material fabrication to define macroporosity and optimize mass transport in, for example, flow battery electrodes.[18,19] Work is also underway to formulate RF and GO precursor solutions for compatibility with advanced manufacturing (3D printing) techniques such as direct ink write and projection microstereo lithography.[20] Lastly, we are continuing to develop novel composite materials based on 3D graphene scaffolds.[21]

Disclosures

The authors have nothing to disclose.

Acknowledgements

This work was performed under the auspices of the U.S. Department of Energy by Lawrence Livermore National Laboratory under Contract DE-AC52-07NA27344. IM release LLNL-JRNL-667016.

References

1. Novoselov, K. S., Geim, A. K., *et al.* Electric field effect in atomically thin carbon films. *Science* **306** (5696), 666-669, (2004).
2. Geim, A. K., & Novoselov, K. S. The rise of graphene. *Nat. Mater.* **6** (3), 183-191, (2007).
3. Li, D., & Kaner, R. B. Materials science. Graphene-based materials. *Science* **320** (5880), 1170-1171, (2008).
4. Allen, M. J., Tung, V. C., & Kaner, R. B. Honeycomb carbon: a review of graphene. *Chem. Rev.* **110** (1), 132-145, (2010).
5. Nardecchia, S., Carriazo, D., Ferrer, M. L., Gutiérrez, M. C., & del Monte, F. Three dimensional macroporous architectures and aerogels built of carbon nanotubes and/or graphene: synthesis and applications. *Chem. Soc. Rev.* **42** (2), 794-830, (2013).
6. Pekala, R. W. Organic aerogels from the polycondensation of resorcinol with formaldehyde. *J. Mater. Sci.* . **24** (9), 3221-3227 (1989).
7. Biener, J., Dasgupta, S., *et al.* Macroscopic 3D nanographene with dynamically tunable bulk properties. *Adv. Mater.* . **24** (37), 5083-5087, (2012).
8. Worsley, M. A., Olson, T. Y., *et al.* High Surface Area, sp 2-Cross-Linked Three-Dimensional Graphene Monoliths. *J Phys. Chem. Lett.* **2** (8), 921-925, (2011).
9. Worsley, M. A., Kucheyev, S. O., *et al.* Mechanically robust 3D graphene macroassembly with high surface area. *Chem Commun*, **48** (67), 8428-8430, (2012).
10. Biener, J., Stadermann, M., *et al.* Advanced carbon aerogels for energy applications. *Energ. Environ. Sci.* **4** (3), 656-667, (2011).
11. Worsley, M. A., Kucheyev, S. O., Satcher, J. H., Hamza, A. V., & Baumann, T. F. Mechanically robust and electrically conductive carbon nanotube foams. *Appl. Phys. Lett.* **94** (7), 073115, (2009).
12. Worsley, M. A., Pauzauskie, P. J., Olson, T. Y., Biener, J., Satcher, J. H., & Baumann, T. F. Synthesis of graphene aerogel with high electrical conductivity. *J. Am. Chem. Soc.* **132** (40), 14067-14069, (2010).
13. Fu, R., Baumann, T. F., Cronin, S., Dresselhaus, G., Dresselhaus, M. S., & Satcher, J. H. Formation of Graphitic Structures in Cobalt- and Nickel-Doped Carbon Aerogels. *Langmuir.* **21** (7), 2647-2651, (2005).
14. Worsley, M. A., Pham, T. T., *et al.* Synthesis and Characterization of Highly Crystalline Graphene Aerogels. *ACS Nano.* **8** (10), 11013-11022, (2014).
15. Campbell, P. G., Merrill, M. D., *et al.* Battery/supercapacitor hybrid via non-covalent functionalization of graphene macro-assemblies. *J. Mater. Chem. A.* **2**, 17764-17770, doi:10.1039/C4TA03605K (2014).
16. Worsley, M. A., Charnvanichborikarn, S., *et al.* Toward Macroscale, Isotropic Carbons with Graphene-Sheet-Like Electrical and Mechanical Properties. *Adv. Funct. Mater.* **24** (27), 4259-4264, (2014).
17. Baumann, T. F., Worsley, M. A., Han, T. Y.-J., & Satcher, J. H., Jr. High surface area carbon aerogel monoliths with hierarchical porosity. *J. Non-Cryst. Solids.* **354** (29), 3513-3515, (2008).
18. Baumann, T. F., & Satcher, J. H., Jr. Template-directed synthesis of periodic macroporous organic and carbon aerogels. *J. Non-Cryst. Solids.* **350**, 120-125, (2004).
19. Braff, W. A., Bazant, M. Z., & Buie, C. R. Membrane-less hydrogen bromine flow battery. *Nat. Comms.* . **4**, 1-6, (2013).
20. Zhu, C., Han, T. Y., Duoss, E. B., Golobic, A. M., Kuntz, J. D., Spadaccini, C. M., & Worsley, M. A. Highly compressible 3D periodic graphene aerogel microlattices, *Nat Comms*, **6**, (2015).
21. Worsley, M. A., Shin, S. J., Merrill, M. D., Lenhardt, J., Nelson, A. J., Woo, L. Y., Gash, A. E., Baumann, T. F., & Orme, C. A. Ultra-Low Density, Monolithic WS_2, MoS_2, and MoS_2 Graphene Aerogels., *ACS Nano.* **9**, (5), 4698-4705, (2015).

